

Effect of removing the no-virtual pair approximation on the correlation energy of the He isoelectronic sequence. II. Point nuclear charge model

Yoshihiro Watanabe,¹ Haruyuki Nakano,^{1,2} and Hiroshi Tatewaki^{3,a)}

¹Department of Chemistry, Faculty of Sciences, Kyushu University, Fukuoka 812-8581, Japan

²CREST, Japan Science and Technology Agency (JST), Kawaguchi, Saitama 332-0012, Japan

³Graduate School of Natural Sciences, Nagoya City University, Nagoya, Aichi 467-8501, Japan

(Received 25 December 2009; accepted 22 February 2010; published online 24 March 2010)

The correlation energies (CEs) of the He isoelectronic sequence $Z=2-116$ with a point nuclear charge model were investigated with the four component relativistic configuration interaction method. We obtained CEs with and without the virtual pair approximation which are close to the values from Pestka *et al.*'s Hylleraas-type configuration interaction calculation. We also found that the uniform charge and point charge models for the nucleus differ substantially for $Z \geq 100$. © 2010 American Institute of Physics. [doi:10.1063/1.3359857]

I. INTRODUCTION

The correlation energy (CE) is defined as the difference between the total energy (TE) calculated with electronic correlations included and that calculated by the Hartree–Fock method. The nonrelativistic CE of the He isoelectronic sequence is almost constant for atoms heavier than ${}_6\text{C}$.^{1–4} In contrast, the relativistic CE of these strongly depends on the atomic number Z . Pestka *et al.*⁵ discovered this using the relativistic Hylleraas-type configuration interaction (Hy-CI) method. Pestka *et al.*,⁶ Tatewaki *et al.*,⁷ and Watanabe *et al.*⁸ found similar Z dependence, using multiconfiguration Dirac–Fock, third-order Douglas–Kroll CI, and four component Dirac–Fock–Roothaan CI (DFR-CI) calculations with DFR $1s_+$ spinor and plural numbers of the s , p , d , and f primitive Gaussian type functions (pGTFs), respectively. The Z dependence of the CE in the latter^{6–8} calculation was stronger than that of Hy-CI.⁵ We shall use the notations TE(I) and CE(I), where I in the parentheses refers to the DFR or the correlated method for calculating the TE and CE: I=DFR-CI or Hy-CI.

We recently showed⁹ that the over estimates of CEs for heavier atoms in the DFR-CI (Ref. 8) were due to the no-virtual pair approximation (NVPA),^{10–12} where excitations to the Dirac negative sea were prohibited. Pestka *et al.*^{13,14} performed unprojected and projected Hy-CI calculations, where the latter uses the Hy-type basis sets giving positive kinetic energies. The projected Hy-CI (Ref. 14) corresponds to the DFR-CI with NVPA, and the unprojected Hy-CI (Ref. 13) corresponds to the DFR-CI with VPA; we shall use the symbol “VPA” when the calculations are performed without NVPA. We abbreviate the TE and CE given by the projected Hy-CI and unprojected Hy-CI to $\text{TE}^{\text{NVPA}}(\text{Hy-CI})$, $\text{CE}^{\text{NVPA}}(\text{Hy-CI})$, $\text{TE}^{\text{VPA}}(\text{Hy-CI})$, and $\text{CE}^{\text{VPA}}(\text{Hy-CI})$, respectively. Using the uniform charge (UC) model for the nucleus, we have found that $\text{CE}^{\text{VPA}}(\text{DFR-CI})$ (Ref. 9) is reasonably parallel to $\text{CE}^{\text{VPA}}(\text{Hy-CI})$,¹³ but the difference between the

two increases as the nuclear charge increases; for example, the difference is 0.4 mhartrees at ${}_{40}\text{Zr}$ and 4.5 mhartrees at ${}_{116}\text{Uuh}$.

The aim of the present work is to obtain the exact TEs under the Dirac–Coulomb Hamiltonian which is widely used in the atomic and molecular electronic calculations, and the quantum electrodynamical terms are not included. The new pGTF basis set is developed for the point nuclear charge model to attain this objective. The TEs by DFR and by DFR-CI are calculated and the resulting CEs are discussed. Almost perfect agreement is found between the $\text{CE}^{\text{VPA}}(\text{Hy-CI})$ and the present $\text{CE}^{\text{VPA}}(\text{DFR-CI})$, and the difference between the $\text{CE}^{\text{NVPA}}(\text{Hy-CI})$ and the present $\text{CE}^{\text{NVPA}}(\text{DFR-CI})$ is analyzed. Since the ground state of the He-like ions are Feshbach resonance state^{15–17} of the electronic states having negative kinetic energies, we discuss the validity of the present results with the stabilization method.^{18–21} Throughout this work we adopt the atomic units.

II. METHOD

The Dirac–Coulomb Hamiltonian is used, where we take the nucleus to be a point charge (PC). The calculation procedure is as follows.

We first determined a universal GTF basis set. An accurate basis set that gives the numerical Dirac–Fock (NDF) limit is needed, since the CE is defined as

$$\text{CE} = \text{TE}(\text{DFR-CI}) - \text{TE}(\text{DFR}). \quad (1)$$

Next, we performed NVPA DFR-CIs with DFR $1s_+$ spinor and s , p , d , f , and g pGTFs, using exponents with coefficients greater than 1×10^{-3} or 1×10^{-2} in the $1s_+$ spinor. The numbers of pGTFs selected vary from one atom to another. For example, these are $(29+1) \times 2$, 29×6 , 29×10 , 29×14 , and 29×18 for s , p , d , f , and g pGTFs for ${}_{116}\text{Uuh}$ if the threshold is 1×10^{-3} , and $(18+1) \times 2$, 18×6 , 18×10 , 18×14 , and 18×18 for s , p , d , f , and g pGTFs if the threshold is 1×10^{-2} (“+1” means that the DFR $1s_+$ spinor is added in case of the s basis set). From the selected

^{a)}Electronic mail: htatewak@nsc.nagoya-cu.ac.jp.

pGTFs, we construct an equal number of orthogonalized spinors for the CI calculations. The total number of spinors for the CI calculations are 1452 and 902, including the $1s_+$ DFR spinor for the smaller and larger threshold, respectively. Five types of CI calculations were performed: s -CI ($1s^2 \rightarrow s's''$), sp -CI ($1s^2 \rightarrow (s' \text{ or } p')(s'' \text{ or } p'')$), spd -CI ($1s^2 \rightarrow (s' \text{ or } p' \text{ or } d')(s'' \text{ or } p'' \text{ or } d'')$), $spdf$ -CI ($1s^2 \rightarrow (s' \text{ or } p' \text{ or } d' \text{ or } f')(s'' \text{ or } p'' \text{ or } d'' \text{ or } f'')$), and $spdfg$ -CI ($1s^2 \rightarrow (s' \text{ or } p' \text{ or } d' \text{ or } f' \text{ or } g')(s'' \text{ or } p'' \text{ or } d'' \text{ or } f'' \text{ or } g'')$). The CE of the respective CIs is given by

$$\text{CE}_i^{\text{NVPA}} = \text{TE}^{\text{NVPA}}(i\text{-CI}) - \text{TE}(\text{DFR}), \quad (2)$$

$$(i = s, sp, spd, spdf, spdfg).$$

The numbers of dimensions for the respective CIs in the case of $_{116}\text{Uuh}$ are 900, 8585, 29 726, 39 083, and 70 480 for the s -, sp -, spd -, $spdf$ -, and $spdfg$ -CI calculations, where the thresholds for selecting the pGTFs are 1×10^{-3} for the first three CI calculations, and for $spdf$ -CI the thresholds are 1×10^{-2} for s , p , and d pGTFs and 1×10^{-3} for f pGTFs; for $spdfg$ -CI the thresholds are 1×10^{-2} for s , p , d , and f pGTFs and 1×10^{-3} for g pGTFs. The accuracy of the $spdf$ - and $spdfg$ -CI can be questioned, but we can safely discuss the resulting CEs resulting from this CI calculation (see below).

To clarify the correlation effects from the s , p , d , f , and g spinors and obtain an accurate TE, we define the partial CE of the s , p , d , f , and g symmetries^{8,9} via the following equations:

$$\begin{aligned} \text{CE}_p^{\text{NVPA}} &= \text{CE}_{sp}^{\text{NVPA}} - \text{CE}_s^{\text{NVPA}}, \\ \text{CE}_d^{\text{NVPA}} &= \text{CE}_{spd}^{\text{NVPA}} - \text{CE}_{sp}^{\text{NVPA}}, \\ \text{CE}_f^{\text{NVPA}} &= \text{CE}_{spdf}^{\text{NVPA}} - \text{CE}_{spd}^{\text{NVPA}}, \\ \text{CE}_g^{\text{NVPA}} &= \text{CE}_{spdfg}^{\text{NVPA}} - \text{CE}_{spdf}^{\text{NVPA}}. \end{aligned} \quad (3)$$

When we calculate $\text{CE}_f^{\text{NVPA}}$ and $\text{CE}_g^{\text{NVPA}}$, we use the pGTFs with a selection threshold of 1×10^{-2} except for the f and g pGTFs, as noted before. For $_{116}\text{Uuh}$, where the truncation error is expected to be greatest, we calculated two $\text{CE}_f^{\text{NVPA}}$ s, one of which is obtained as defined above and the other from the basis set with a threshold of 1×10^{-3} used for all the symmetries s - f . The difference between the two $\text{CE}_f^{\text{NVPA}}$ s is 0.0000 36 mhartrees, confirming that the error in evaluating $\text{CE}_f^{\text{NVPA}}$ if the truncated s , p , and d basis sets are used is small. We expect the calculated $\text{CE}_g^{\text{NVPA}}$ to have high accuracy, as in the case of $\text{CE}_f^{\text{NVPA}}$. From these equations we have

$$\text{TE}^{\text{NVPA}}(\text{DFR-CI}) = \text{TE}(\text{DFR}) + \text{CE}^{\text{NVPA}},$$

where

$$\text{CE}^{\text{NVPA}} = \sum_{i=s}^g \text{CE}_i^{\text{NVPA}}. \quad (4)$$

The $\text{TE}^{\text{NVPA}}(\text{DFR-CI})$ is obtained from Eq. (4), where $\text{CE}_{i=f,g}^{\text{NVPA}}$ is calculated using smaller basis sets.

Thirdly DFR-CI calculation without NVPA is performed using a modified DFR-CI program,²² where DFR spinors

TABLE I. TE by DFR and CEs, CE^{NVPA} and CE^{VPA} , from CI with the s , p , d , f , and g spinors in hartrees.

Z	TE(DFR)	NVPA	VPA
2	-2.861 813	-0.041 838	-0.041 838
3	-7.237 206	-0.043 221	-0.043 221
4	-13.614 001	-0.043 947	-0.043 946
5	-21.993 149	-0.044 386	-0.044 386
6	-32.375 989	-0.044 679	-0.044 677
7	-44.764 201	-0.044 886	-0.044 883
8	-59.159 794	-0.045 039	-0.045 033
9	-75.565 105	-0.045 155	-0.045 146
10	-93.982 800	-0.045 246	-0.045 232
11	-114.415 873	-0.045 317	-0.045 299
12	-136.867 655	-0.045 376	-0.045 349
13	-161.341 806	-0.045 423	-0.045 388
14	-187.842 329	-0.045 462	-0.045 417
15	-216.373 565	-0.045 494	-0.045 437
16	-246.940 200	-0.045 522	-0.045 450
17	-279.547 271	-0.045 546	-0.045 457
18	-314.200 165	-0.045 567	-0.045 460
19	-350.904 626	-0.045 585	-0.045 457
20	-389.666 763	-0.045 602	-0.045 449
21	-430.493 051	-0.045 618	-0.045 439
22	-473.390 336	-0.045 633	-0.045 424
23	-518.365 844	-0.045 648	-0.045 407
24	-565.427 188	-0.045 663	-0.045 386
25	-614.582 370	-0.045 678	-0.045 363
26	-665.839 791	-0.045 694	-0.045 338
27	-719.208 260	-0.045 711	-0.045 309
28	-774.696 997	-0.045 729	-0.045 279
29	-832.315 648	-0.045 749	-0.045 245
30	-892.074 289	-0.045 770	-0.045 211
31	-953.983 434	-0.045 793	-0.045 175
32	-1018.054 051	-0.045 818	-0.045 136
33	-1084.297 567	-0.045 846	-0.045 095
34	-1152.725 881	-0.045 875	-0.045 054
35	-1223.351 374	-0.045 907	-0.045 011
36	-1296.186 924	-0.045 941	-0.044 968
37	-1371.245 915	-0.045 979	-0.044 925
38	-1448.542 253	-0.046 019	-0.044 876
39	-1528.090 380	-0.046 063	-0.044 824
40	-1609.905 287	-0.046 109	-0.044 775
41	-1694.002 532	-0.046 159	-0.044 726
42	-1780.398 253	-0.046 212	-0.044 685
43	-1869.109 190	-0.046 269	-0.044 624
44	-1960.152 698	-0.046 331	-0.044 564
45	-2053.546 771	-0.046 395	-0.044 511
46	-2149.310 059	-0.046 464	-0.044 457
47	-2247.461 889	-0.046 537	-0.044 402
48	-2348.022 289	-0.046 615	-0.044 348
49	-2451.012 013	-0.046 697	-0.044 294
50	-2556.452 560	-0.046 784	-0.044 232
51	-2664.366 208	-0.046 876	-0.044 175
52	-2774.776 033	-0.046 973	-0.044 119
53	-2887.705 947	-0.047 074	-0.044 064
54	-3003.180 723	-0.047 182	-0.044 010
55	-3121.226 026	-0.047 294	-0.043 954
56	-3241.868 455	-0.047 414	-0.043 892
57	-3365.135 570	-0.047 538	-0.043 838
58	-3491.055 938	-0.047 669	-0.043 785

TABLE I. (Continued.)

Z	TE(DFR)	NVPA	VPA
59	-3619.659 168	-0.047 806	-0.043 733
60	-3750.975 957	-0.047 950	-0.043 687
61	-3885.038 136	-0.048 100	-0.043 639
62	-4021.878 716	-0.048 258	-0.043 586
63	-4161.531 939	-0.048 423	-0.043 539
64	-4304.033 336	-0.048 596	-0.043 497
65	-4449.419 779	-0.048 776	-0.043 423
66	-4597.729 550	-0.048 965	-0.043 377
67	-4749.002 397	-0.049 161	-0.043 334
68	-4903.279 611	-0.049 368	-0.043 306
69	-5060.604 098	-0.049 583	-0.043 245
70	-5221.020 454	-0.049 807	-0.043 218
71	-5384.575 056	-0.050 042	-0.043 195
72	-5551.316 147	-0.050 286	-0.043 184
73	-5721.293 932	-0.050 542	-0.043 152
74	-5894.560 687	-0.050 809	-0.043 134
75	-6071.170 860	-0.051 087	-0.043 113
76	-6251.181 199	-0.051 378	-0.043 096
77	-6434.650 872	-0.051 681	-0.043 106
78	-6621.641 606	-0.051 997	-0.043 105
79	-6812.217 837	-0.052 328	-0.043 088
80	-7006.446 863	-0.052 673	-0.043 101
81	-7204.399 017	-0.053 033	-0.043 121
82	-7406.147 856	-0.053 409	-0.043 149
83	-7611.770 352	-0.053 802	-0.043 187
84	-7821.347 116	-0.054 213	-0.043 195
85	-8034.962 629	-0.054 643	-0.043 201
86	-8252.705 496	-0.055 092	-0.043 275
87	-8474.668 726	-0.055 561	-0.043 391
88	-8700.950 032	-0.056 053	-0.043 486
89	-8931.652 160	-0.056 568	-0.043 585
90	-9166.883 251	-0.057 108	-0.043 679
91	-9406.757 237	-0.057 673	-0.043 815
92	-9651.394 272	-0.058 265	-0.043 923
93	-9900.921 208	-0.058 887	-0.044 094
94	-10 155.472 123	-0.059 542	-0.044 275
95	-10 415.188 900	-0.060 228	-0.044 445
96	-10 680.221 868	-0.060 949	-0.044 649
97	-10 950.730 516	-0.061 709	-0.044 863
98	-11 226.884 284	-0.062 511	-0.045 194
99	-11 508.863 446	-0.063 356	-0.045 453
100	-11 796.860 100	-0.064 247	-0.045 751
101	-12 091.079 274	-0.065 189	-0.046 088
102	-12 391.740 175	-0.066 187	-0.046 531
103	-12 699.077 592	-0.067 243	-0.046 990
104	-13 013.343 489	-0.068 364	-0.047 428
105	-13 334.808 819	-0.069 554	-0.047 914
106	-13 663.765 581	-0.070 822	-0.048 556
107	-14 000.529 188	-0.072 172	-0.049 292
108	-14 345.441 188	-0.073 613	-0.049 929
109	-14 698.872 397	-0.075 154	-0.050 615
110	-15 061.226 553	-0.076 808	-0.051 423
111	-15 432.944 569	-0.078 583	-0.052 374
112	-15 814.509 526	-0.080 495	-0.053 351
113	-16 206.452 571	-0.082 560	-0.054 544
114	-16 609.359 921	-0.084 795	-0.055 755
115	-17 023.881 245	-0.087 221	-0.057 130
116	-17 450.739 770	-0.089 868	-0.058 641

with negative kinetic energies are utilized; for example, we performed CI with $1s^2 \rightarrow s's''$, where s' and s'' include spinors with positive and negative kinetic energies. The total number of GTFs used is twice that of the NVPA calculations; in the case of ${}_{116}\text{Uuh}$ there are 2904 and 1804 GTFs for the smaller and larger thresholds, respectively. Equations parallel to (2) and (3) are obtained for the case of VPA. Here, we only write the equation corresponding to Eq. (4)

$$\text{TE}^{\text{VPA}}(\text{DFR-CI}) = \text{TE}(\text{DFR}) + \text{CE}^{\text{VPA}}$$

and

$$\text{CE}^{\text{VPA}} = \sum_{i=s}^g \text{CE}_i^{\text{VPA}}. \quad (5)$$

To obtain CE^{VPA} it is necessary to perform s -, sp -, spd -, $spdf$ -, and $spdfg$ -CI calculations with VPA. We were able to handle s - and sp -CI calculations having dimensions 3600 and 34 300, respectively, but could not perform spd -, $spdf$ -, and $spdfg$ -CI calculations since the dimension of the Hamiltonian matrix becomes large. We can obtain CE_s^{VPA} and CE_p^{VPA} but not $\text{CE}_{i=d,f,g}^{\text{VPA}}$. Instead of directly calculating $\text{CE}_{i=d,f,g}^{\text{VPA}}$, we introduce $\delta\text{CE}_{i=d,f,g}$ as given below

$$\begin{aligned} \delta\text{CE}_d &= \text{CE}_d^{\text{VPA}} - \text{CE}_d^{\text{NVPA}} \\ &= \text{CE}_{spd}^{\text{VPA}} - \text{CE}_{sp}^{\text{VPA}} - (\text{CE}_{spd}^{\text{NVPA}} - \text{CE}_{sp}^{\text{NVPA}}) \\ &\approx \text{CE}_{sd}^{\text{VPA}} - \text{CE}_s^{\text{VPA}} - (\text{CE}_{sd}^{\text{NVPA}} - \text{CE}_s^{\text{NVPA}}) \\ &= \text{CE}_{sd}^{\text{VPA}} - \text{CE}_{sd}^{\text{NVPA}} - (\text{CE}_s^{\text{VPA}} - \text{CE}_s^{\text{NVPA}}) \\ &= \text{CE}_{sd}^{\text{VPA}} - \text{CE}_{sd}^{\text{NVPA}} - \delta\text{CE}_s. \end{aligned} \quad (6)$$

Likewise we have

$$\delta\text{CE}_f = \text{CE}_{sf}^{\text{VPA}} - \text{CE}_{sf}^{\text{NVPA}} - \delta\text{CE}_s,$$

and

$$\delta\text{CE}_g = \text{CE}_{sg}^{\text{VPA}} - \text{CE}_{sg}^{\text{NVPA}} - \delta\text{CE}_s. \quad (7)$$

Here, we calculate sd -, sf -, and sg -CIs instead of spd -, $spdf$ -, and $spdfg$ -CIs; for ${}_{116}\text{Uuh}$ we found that the approximation in the third row of Eq. (6) gives an error of 0.018 mhartrees relative to δCE_d given by VPA sp - and spd -CIs with a truncation threshold of 1×10^{-3} . We can disregard this small error of the order 0.01 mhartrees when δCE_d is calculated. We also expect smaller errors than this for $\delta\text{CE}_{i=f,g}$. The dimensions of sd -, sf -, and sg -CIs in the space VPA are 47 796, 61 252, and 74 708, whereas those in NVPA are 11 949, 15 313, and 18 677. We obtain CE_d^{VPA} , CE_f^{VPA} , and CE_g^{VPA} in Eq. (5) as

$$\text{CE}_i^{\text{VPA}} = \text{CE}_i^{\text{NVPA}} + \delta\text{CE}_i (i = d, f, \text{ and } g). \quad (8)$$

Using Eqs. (5) and (8), we now obtain TE^{VPA} without calculating spd -, $spdf$ -, and $spdfg$ -CI.

III. RESULTS AND DISCUSSION

A. Basis set

The CE of the He-like ions was considered up to ${}_{116}\text{Uuh}$. We first applied the previous universal-like GTFs^{8,9} for the UC model to calculate the He-like ions with the PC model.

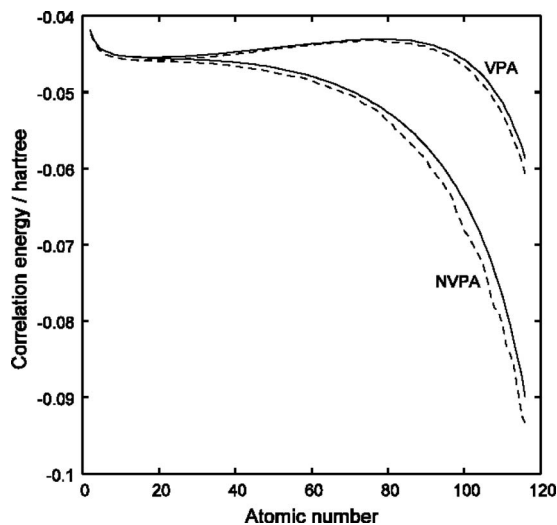


FIG. 1. CEs in hartrees. Solid lines: $CE^{NVPA}(\text{DFR-CI})$ and $CE^{VPA}(\text{DFR-CI})$ with s, p, d, f, g pGTFs; dashed lines: $CE^{NVPA}(\text{Hy-CI})$ and $CE^{VPA}(\text{Hy-CI})$ calculated from Refs. 14 and 13, respectively.

The errors in TE(DFR) with the PC model are less than 0.408 hartrees, but they are large if we compare them with those ($<0.01 \mu\text{hartrees}$) from the UC model. They are not sufficiently accurate to calculate the CE given by Eq. (1), where TE(DFR) is required to have the NDF accuracy. We therefore develop new even-tempered basis sets. After several test calculations, the range of exponents was found to lie between 4.00×10^{-2} and 1.60×10^{22} , where the largest exponent is 4.7×10^{10} times larger than that of the UC model (exponents for the UC model are between 5.88×10^{-2} and 3.37×10^{11}). The test basis set was composed of 90 functions where even-tempered exponents are assumed. The errors in TE(DFR) calculated with this set from TE(NDF) are less than $1.0 \mu\text{hartrees}$ for all atomic ions considered. We found that a plot of CE versus the atomic number Z has anomalies, however: a sharp increase and a sharp decrease in the CE are observed at several atoms. We suspect that this is due to insufficiency in the number of the basis set. The exponent parameters in even-tempered basis sets are determined by Eq. (9). We increase the number of a basis set by changing β where we fix $\alpha=0.04$. We finally settle on a universal set composed of 136 s -type pGTFs, where β is close to 1.5 and near to the value used in the Refs. 8 and 9

$$\zeta_n = \alpha\beta^{n-1} \quad (\alpha=0.04, \beta=1.495650, n=1, \dots, 136). \quad (9)$$

The errors in TE(DFR) calculated with this set from TE(NDF) are again less than $1.0 \mu\text{hartrees}$, but we found no difficulties in calculating CEs as in the case of 90 expansion terms. This sequence is also used for the $p, d, f,$ and g spinors.

B. CE with NVPA

We performed NVPA DFR-CIs with DFR $1s_+$ spinor and $s, p, d, f,$ and g pGTFs, with exponents having coefficients greater than 1×10^{-3} or 1×10^{-2} in the $1s_+$ spinor, following the discussion relating to Eqs. (3) and (4). The TE(DFR) and $CE^{NVPA}(\text{DFR-CI})$ given by Eq. (4) with $s, p, d, f,$ and g

spinor sets are set out in Table I, together with $CE^{VPA}(\text{DFR-CI})$, which will be discussed below. Figure 1 also shows $CE^{NVPA}(\text{DFR-CI})$ and $CE^{NVPA}(\text{Hy-CI})$ together with two CE^{VPA} s.

We see that the present two $CE^{NVPA}(\text{DFR-CI})$ s and $CE^{NVPA}(\text{Hy-CI})$ decrease sharply as the atomic number Z increases. The difference between the $spdfg$ -CI and the Hy-CI CE^{NVPA} s begins from 0.20 mhartrees at ${}_2\text{He}$ and reaches 3.46 mhartrees at ${}_{116}\text{Uuh}$. We now discuss these differences. The partial CEs in NVPA, CE_i^{NVPA} s are set out in Figs. 2(a) and 2(b). The CE_s^{NVPA} changes sharply as Z increases; it has a maximum of -14.7 mhartrees at ${}_{16}\text{S}$ and a minimum of -54.7 mhartrees at ${}_{116}\text{Uuh}$. The changes in $CE_s^{NVPA}(\text{DFR-CI})$ reach 40.0 mhartrees. CE_p^{NVPA} has a maximum of -21.5 mhartrees at ${}_2\text{He}$ and a minimum of -29.1 mhartrees at ${}_{116}\text{Uuh}$, where the change in CE_p^{NVPA} is 7.6 mhartrees. On the other hand, $CE_{i \geq 2}^{NVPA}$ changes moderately when Z increases: (1) CE_d^{NVPA} has a maximum of -2.3 mhartrees at ${}_2\text{He}$ and a minimum of -4.3 mhartrees at ${}_{116}\text{Uuh}$, where the change in CE_d^{NVPA} is 2.0 mhartrees, 5% of CE_s^{NVPA} ; (2) the CE_f^{NVPA} has a maximum of -0.6 mhartrees at ${}_2\text{He}$ and a minimum of -1.3 mhartrees at ${}_{116}\text{Uuh}$; and (3) the CE_g^{NVPA} has a maximum of -0.2 mhartrees at ${}_2\text{He}$ and a minimum of -0.6 mhartrees at ${}_{116}\text{Uuh}$, where the change in CE_f^{NVPA} is 0.4 mhartrees, 1% part of CE_s^{NVPA} . We recall that the difference between $CE^{NVPA}(\text{DFR-CI})$ and $CE^{NVPA}(\text{Hy-CI})$ reaches 3.46 mhartrees for ${}_{116}\text{Uuh}$. Variation in CE_i^{NVPA} as Z increases flatters out. If we further take account of the CEs from the correlating orbitals with beyond g , it becomes difficult to explain the differences between $CE^{NVPA}(\text{DFR-CI})$ and $CE^{NVPA}(\text{Hy-CI})$; geometrical extrapolation gives

$$CE_{s,p,d,\dots,\infty}^{NVPA} = CE_s^{NVPA} + CE_p^{NVPA} + CE_d^{NVPA} + CE_f^{NVPA} / (1 - CE_g^{NVPA}/CE_f^{NVPA}). \quad (10)$$

$CE_{s,p,d,\dots,\infty}^{NVPA}$ is -90.28 mhartrees at ${}_{116}\text{Uuh}$, and we still have a discrepancy of 3.05 mhartrees [$CE^{NVPA}(\text{Hy-CI})$: -93.33 mhartrees].

Since the changes in CE_s^{NVPA} versus Z are large, use of the truncated s spinor set appears likely to be responsible for the large differences between $CE^{NVPA}(\text{DFR-CI})$ and $CE^{NVPA}(\text{Hy-CI})$. We, tested this, however, when we adopted the threshold for truncation of the basis set; for ${}_{116}\text{Uuh}$, where the maximum difference is expected, $\text{TE}(s\text{-CI with truncated } 30 \times 2 \text{ spinors}) = -17450.794428$ and also $\text{TE}(s\text{-CI with full } 136 \times 2 \text{ spinors}) = -17450.794428$, both of which give CE_s^{NVPA} of -54.658 mhartrees. The same is true for all of the atoms. For CE_p^{NVPA} , we had calculated two CE_p^{NVPA} values. For ${}_{116}\text{Uuh}$, one of these is obtained by CI with TE(s 30×2 spinors with threshold 1×10^{-3} and p 29×6 spinors with threshold 1×10^{-3}), and the other is CI with TE(s 30×2 spinors with threshold 1×10^{-3} and p 53×6 spinors with threshold 1×10^{-5}). The former gives $CE_p^{NVPA} = -29.066$ mhartrees and the latter -29.077 mhartrees. Enlarging the p basis set scarcely

changes the CE_p^{NVPA} values by mhartrees. We see that truncation in the s and p sets is not responsible for the large difference between $CE^{\text{NVPA}}(\text{DFR-CI})$ and $CE^{\text{NVPA}}(\text{Hy-CI})$ which is 1–5 mhartrees beyond $_{80}\text{Hg}$. We also infer that the correlating spinors with higher angular momentum ($\geq h$) are not responsible for the difference between the two CE^{NVPA}_s . Using numerical multiconfiguration self-consistent-field with higher angular momentum spinors ($l=7$) and the extrapolation, Parpia *et al.*²³ have obtained CE^{NVPA} for He-like ions ($Z=1-26$) with infinite spinors. Their extrapolated value for $_{26}\text{Fe}^{24+}$ is -45.8 mhartrees which is close to our CE_{spdfg}^{NVPA} value of -45.7 and -45.9 mhartrees of the extrapolated value given by Eq. (10), confirming the accuracy of the present CE^{NVPA} values.

Sapirstein *et al.*²⁴ have shown that TE^{NVPA}_s obtained by CI calculations depend on the electronic potential adopted, namely, depend on the resulting spinors and resulting CSFs; the size of the CI space for NVPA practically changes according to the electronic potential adopted. Their result also suggests that CE^{NVPA}_s depend on the functional form to construct the NVPA CI space. The disagreement between $CE^{\text{NVPA}}(\text{Hy-CI})$ and $CE^{\text{NVPA}}(\text{DFR-CI})$ is therefore accepted, even though the two calculations use fairly large basis sets, since the NVPA CI spaces spanned by the spinors or Hy functions with positive kinetic energies are expected to be different. Without NVPA, the disagreement between $CE(\text{Hy-CI})$ and $CE(\text{DFR-CI})$ should be smaller, since the spaces generated with the full basis functions with the positive and negative kinetic energies (the complete CI) are used.

C. CE without NVPA

We calculate VPA DFR-CI, where three kinds of CSFs are constructed from a pair of spinors with positive or negative kinetic energy. Upon adapting the Davidson's diagonalization method,^{25,26} we directly obtained the solution for which the main CSF is the DFR $1s_+^2$.

To simplify the larger calculations involved in considering spinors with negative kinetic energies, we used Eqs. (5)–(8). In calculating δCE_d , the errors caused by the approximation at third line in Eq. (6) were less than 0.018 mhartrees for $_{116}\text{Uuh}$, as discussed. We expect the error in $\delta CE_{i>d}$ due to this approximation to be smaller still.

The calculated CE^{VPA}_s , the sums of the $CE_i^{\text{VPA}}_s$ have been set out in Table I and in Fig. 1. Figure 1 shows that $CE^{\text{VPA}}(\text{DFR-CI})$ by *spdfg*-CI are almost in agreement with $CE^{\text{VPA}}(\text{Hy-CI})$, indicating the good choice of the approximations in Sec. II. The agreement of $CE^{\text{VPA}}(\text{DFR-CI})$ with $CE^{\text{VPA}}(\text{Hy-CI})$ also indicates that the CE^{VPA}_s are independent of the methodology to determine the CI space.

Let us discuss the details of CE^{VPA} . The partial CEs $CE_i^{\text{VPA}}_s$ are shown in Figs. 2(a) and 2(b) together with $CE_i^{\text{NVPA}}_s$. Figure 2(a) shows that CE_s^{VPA} is greater than CE_s^{NVPA} , but it also shows that CE_s^{VPA} decreases sharply as CE_s^{NVPA} . CE_s^{VPA} has a maximum of -14.7 mhartrees at $_{16}\text{S}$ and a minimum of -44.4 mhartrees at $_{116}\text{Uuh}$. We recall that CE_s^{NVPA} has a maximum of -14.7 mhartrees at $_{16}\text{S}$ and a minimum of -54.7 mhartrees at $_{116}\text{Uuh}$.

On the basis of the second order perturbation theory, CE_i^{VPA} is given approximately by

$$\begin{aligned}
 CE_i^{\text{VPA}} \approx & \\
 & - \sum_{\kappa', \kappa''}^{I_1: \varepsilon(\kappa') > 0, \varepsilon(\kappa'') > 0} |\langle \Phi(\text{DFR} - 1s^2) | H | \Phi(1s^2 \rightarrow \kappa' \kappa'') \rangle|^2 / (E_{i(\kappa', \kappa'')} - E_0) \\
 & + \sum_{\kappa', \kappa''}^{I_2 \notin I_1} |\langle \Phi(\text{DFR} - 1s^2) | H | \Phi(1s^2 \rightarrow \kappa' \kappa'') \rangle|^2 / (E_0 - E_{i(\kappa', \kappa'')}), \quad (11)
 \end{aligned}$$

where i denotes the symmetry to which the spinors κ' and κ'' belong. The first term gives the approximate value of CE_i^{NVPA} where the spinor energies are calculated with positive kinetic energies, and the second term gives the approximate value for the partial virtual pair correction (ΔCE_i^{VPA}) arising from the configurations with the spinors, at least, one of which has negative kinetic energy. ΔCE_i^{VPA} is positive so that the CE_i^{VPA} is greater than CE_i^{NVPA} . We define the (total) virtual pair correction ΔCE^{VPA} as $\sum_i \Delta CE_i^{\text{VPA}}$ which denotes the coupling between the positive and negative states (often called the Brown–Ravenhall continuum) through electron-electron interaction.

In contrast to CE_s^{VPA} , which has a maximum at $_{16}\text{S}$ and then decreases as Z increases, the other $CE_{i \geq 1}^{\text{VPA}}$ s have a mini-

um between $_{15}\text{P}$ and $_{18}\text{Ar}$ and then increase monotonically, indicating that ΔCE_i^{VPA} is important for $i \geq p$. The (absolute) CE_i^{VPA} values are fairly small compared to (absolute) CE_s^{VPA} values except for CE_p^{VPA} . At $_{116}\text{Uuh}$, CE_i^{VPA} are -18.1 , 1.0 , 1.5 , and 1.3 mhartrees for $i=p, d, f$, and g respectively, compared to $CE_s^{\text{VPA}} = -44.4$ mhartrees. We realize that CE^{VPA} is governed by CE_s^{VPA} and CE_p^{VPA} . In total, $CE^{\text{VPA}} = -58.6$ mhartrees for $_{116}\text{Uuh}$ and the $CE^{\text{NVPA}} = -89.9$ mhartrees. The partial virtual pair corrections, ΔCE_i^{VPA} given by $CE_i^{\text{VPA}} - CE_i^{\text{NVPA}}$ are 10.3 , 10.9 , 5.3 , 2.8 , and 1.9 mhartrees for $i=s, p, d, f$, and g .

We recall that CE^{NVPA} and CE^{VPA} values for $_{116}\text{Uuh}$ by Hy-CI were, respectively, -93.3 and -60.7 mhartrees compared to the corresponding values of -89.9 and -58.6 mhar-

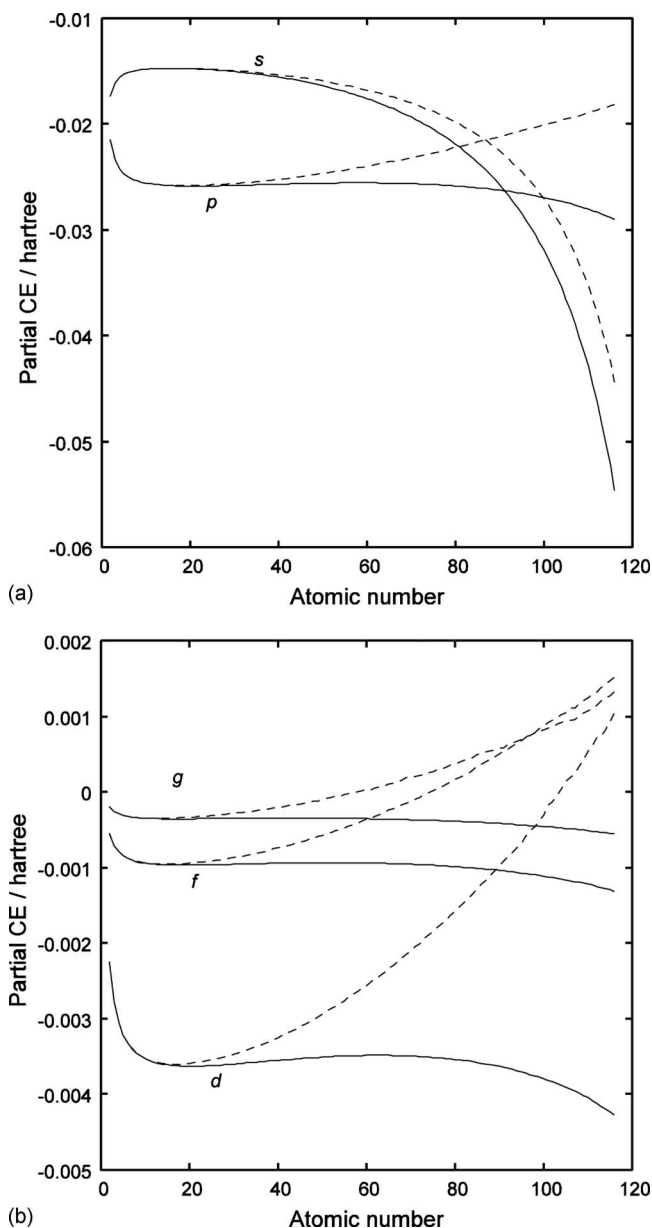


FIG. 2. (a) Partial CEs in hartrees. Solid lines: $CE_i^{NVPA}(i=s,p)$; and dashed lines: $CE_i^{VPA}(i=s,p)$. (b) Partial CEs in hartrees. Solid lines: $CE_i^{NVPA}(i=d,f,g)$; and dashed lines: $CE_i^{VPA}(i=d,f,g)$.

trees. The difference in CE^{VPA} is small compared with that in CE^{NVPA} since in VPA the CI space is a full space spanned by the spinors or Hy functions with the positive and negative kinetic energies.

We here compare the present $\delta CE(s)$, $\delta CE(p)$, and $\delta CE(d)$ values for ${}_{92}\text{U}$ with those of Sapirstein *et al.*²⁴ Their values, which are calculated by a similar CI method to the present one on the basis of the B-spline method with the PC model, are 3.4, 5.5, and 2.8 mhartrees for $\delta CE(s)$, $\delta CE(p)$, and $\delta CE(d)$, respectively, whereas our present calculations with the point nuclear charge model gave 3.4, 5.4, and 2.8 mhartrees. Complete agreement is observed, in contrast to our previous calculation with the UC model, giving 3.1, 5.0, and 2.6 mhartrees.

We finally show that the $1s^2$ discussed corresponds to Feshbach resonance state. The stabilization method is em-

ployed to show this. In the stabilization method, the several configurations are chosen as the initial wavefunction of the quasibound state. This is then improved by adding more configurations until it is observed that one root and one trial function is no longer affected by the addition of any bound configurations with which it could mix. The root is termed stabilized and taken as the resonant wavefunction.^{18–21} In order to verify $1s^2$ is the Feshbach resonance state we only consider $1s^2(\text{KE} > 0) \rightarrow s's''\text{CI}$, since the resources for the computation are limited and the largest contribution in CE arises from the $1s^2(\text{KE} > 0) \rightarrow s's''\text{CI}$. To specify the $1s^2$ state with the positive kinetic energy from that of the negative kinetic energy, the notations $1s^2(\text{KE} > 0)$ and $1s^2(\text{KE} < 0)$ are used. We consider ${}_{116}\text{Uuh}$. The $1s^2(\text{KE} > 0)$ is definitely chosen as the initial wavefunction of the quasibound state. The sizes of the basis function are 5×4 , 10×4 , 15×4 , 20×4 , 30×4 , 60×4 , 90×4 , 100×4 , 110×4 , 120×4 , 130×4 , and 136×4 , where 4 implies $ns(\text{KE} > 0)$, $\underline{ns}(\text{KE} > 0)$, $ns(\text{KE} < 0)$, and $\underline{ns}(\text{KE} < 0)$ are employed; \underline{ns} is a Kramers' partner of ns . The dimension of the CI is $(n \times 4)^2$. The resulting TEs are $-0.041\ 651$, $-0.044\ 546$, $-0.044\ 404$, $-0.044\ 370$, $-0.044\ 364$, $-0.044\ 375$, $-0.044\ 376$, $-0.044\ 376$, $-0.044\ 376$, $-0.044\ 376$, and $-0.044\ 376$ relative to the DFR value of $-17\ 450.739\ 770$ hartrees. We see the perfect stabilization and the state is the resonance state. Since the state $1s^2(\text{KE} > 0)$ is the two electron excited state relative to $1s^1(\text{KE} < 0) + e$, the state $1s^2(\text{KE} > 0)$ is inferred as the type of the Feshbach resonance.

D. CEs calculated with different nucleus models

Figure 3 shows CE differences between the point nuclear charge model and the UC nucleus models of the previous calculations^{8,9} in the case of *spdf*-CI. The CE differences

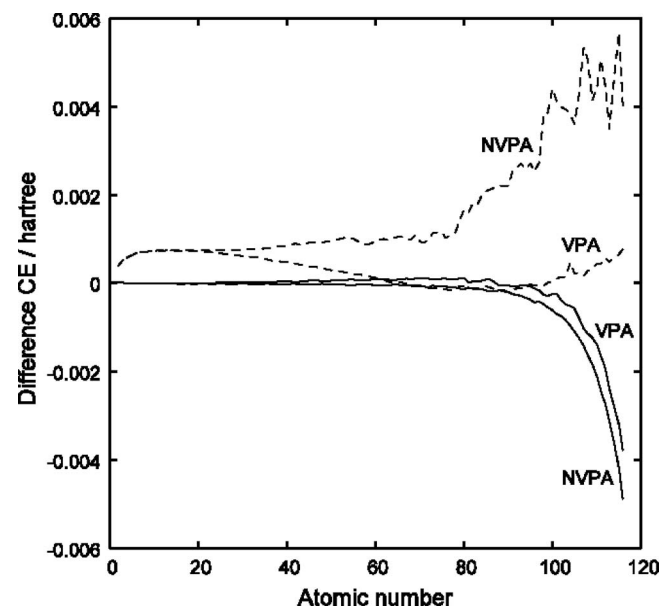


FIG. 3. Comparison of the CEs calculated with the PC and UC models of the nucleus; the *s*, *p*, *d*, and *f* spinors are used to obtain CEs. Solid lines: $CE^X(\text{PC}) - CE^X(\text{UC})$; dashed lines: $CE^X(\text{PC}) - CE^X(\text{Hy-CI})$; and $X = \{\text{NVPA or VPA}\}$. The $CE^X(\text{UC})$ is calculated from Refs. 8 and 9. The $CE^X(\text{Hy-CI})$ are calculated from Refs. 14 and 13.

TABLE II. CEs calculated by Hy-CI and by DFR-CI with s , p , d , and f spinors, using the PC and UC models of the nucleus, in mhartrees.

Z	CE ^{NVPA}			CE ^{VPA}		
	Hy-CI	DFR-CI ^{PC}	DFR-CI ^{UC}	Hy-CI	DFR-CI ^{PC}	DFR-CI ^{UC}
2	-42.044	-41.640	-41.644	-42.043	-41.640	-41.644
10	-45.624	-44.896	-44.883	-45.611	-44.885	-44.873
20	-45.989	-45.245	-45.235	-45.825	-45.113	-45.112
30	-46.169	-45.419	-45.403	-45.541	-44.925	-44.936
40	-46.613	-45.761	-45.726	-45.043	-44.568	-44.602
50	-47.390	-46.435	-46.407	-44.430	-44.130	-44.174
60	-48.533	-47.593	-47.548	-43.833	-43.708	-43.777
70	-50.376	-49.438	-49.364	-43.346	-43.409	-43.516
80	-53.927	-52.283	-52.153	-43.387	-43.473	-43.582
90	-58.889	-56.689	-56.474	-44.039	-44.253	-44.202
100	-68.200	-63.789	-63.172	-46.600	-46.574	-46.332
105	-72.681	-69.071	-67.991	-49.081	-48.847	-48.266
110	-80.747	-76.295	-74.173	-52.947	-52.499	-51.117
116	-93.329	-89.311	-84.423	-60.729	-59.961	-56.187

between the $spdf$ -CI and Hy-CI^{13,14} in the point nuclear charge model are also included. Table II shows these CEs for selected ions, since the figure shows only the differences of CEs versus Z . The differences in CE^{NVPA}s according to the two nuclear models are considerable for $Z \geq 100$; the changes in the CEs depend on the models of the nucleus, although the differences are small. We again see that the VPA CEs given by DFR-CI are close to those by Hy-CI.

IV. CONCLUSION

We investigated the CEs of the He isoelectronic sequence $Z=2-116$ with a PC model of the nucleus using the four component relativistic CI method. We obtained CEs with and without the virtual pair approximation which are close to the values from Pestka *et al.*'s Hylleraas-type CI (Hy-CI); for ${}_{116}\text{Uuh}$, the CE with and without virtual pair approximations using the present CI are, respectively, -89.9 and -58.6 mhartrees, which correspond to those of Hy-CI, -93.3 (Ref. 14) and -60.7 mhartrees.¹³ Relatively large CE differences between DFR-CI and Hy-CI without the virtual pair are attributed to the differences of the method to construct the CI space with positive kinetic energies.

ACKNOWLEDGMENTS

This study was partly supported by Grants-in-Aid for Scientific Research to one of the authors (H.T.) from the Ministry of Education, Culture, Sports, Science and Technology of Japan (Grant No. 16080216).

- ¹E. Clementi, *J. Chem. Phys.* **38**, 2248 (1963).
- ²J. Midtdal and K. Aashanar, *Phys. Norv.* **2**, 99 (1967).
- ³G. W. Drake, *Can. J. Phys.* **66**, 586 (1988).
- ⁴E. R. Davidson, S. A. Hagstrom, and S. J. Chakravorty, *Phys. Rev. A* **44**, 7071 (1991).
- ⁵G. Pestka and J. Karwowski, in *Explicitly Correlated Wavefunctions in Chemistry and Physics*, edited by J. Rychlewski (Kluwer Academic, Dordrecht, 2003), p. 331.
- ⁶G. Pestka, H. Tatewaki, and J. Karwowski, *Phys. Rev. A* **70**, 024501 (2004).
- ⁷H. Tatewaki and T. Noro, *Chem. Phys. Lett.* **399**, 480 (2004).
- ⁸Y. Watanabe and H. Tatewaki, *J. Chem. Phys.* **123**, 074322 (2005).
- ⁹Y. Watanabe, H. Nakano, and H. Tatewaki, *J. Chem. Phys.* **126**, 174105 (2007).
- ¹⁰G. E. Brown and D. G. Ravenhall, *Proc. R. Soc. London Ser. A* **208**, 552 (1951).
- ¹¹M. H. Mittleman, *Phys. Rev. A* **4**, 893 (1971).
- ¹²J. Sucher, *Phys. Rev. A* **22**, 348 (1980).
- ¹³G. Pestka, M. Bylicki, and J. Karwowski, *J. Phys. B* **40**, 2249 (2007).
- ¹⁴M. Bylicki, G. Pestka, and J. Karwowski, *Phys. Rev. A* **77**, 044501 (2008).
- ¹⁵G. J. Schulz, *Rev. Mod. Phys.* **45**, 378 (1973).
- ¹⁶G. J. Schulz, *Rev. Mod. Phys.* **45**, 423 (1973).
- ¹⁷P. G. Burke, *Adv. Phys.* **14**, 521 (1965).
- ¹⁸L. Lipsky and A. Russek, *Phys. Rev.* **142**, 59 (1966).
- ¹⁹F. Holøien and J. Midtdal, *J. Chem. Phys.* **45**, 2209 (1966).
- ²⁰H. S. Taylor, G. V. Nazaoff, and A. Golebiewski, *J. Chem. Phys.* **45**, 2872 (1966).
- ²¹I. Eliezer and Y. K. Pan, *Theor. Chim. Acta* **16**, 63 (1970).
- ²²Y. Watanabe and O. Matsuoka, *J. Chem. Phys.* **116**, 9585 (2002).
- ²³F. A. Parpia, and I. P. Grant, *J. Phys. B* **23**, 211 (1990).
- ²⁴J. Sapirstein, K. T. Cheng, and M. H. Chen, *Phys. Rev. A* **59**, 259 (1999).
- ²⁵E. R. Davidson, *J. Comput. Phys.* **17**, 87 (1975).
- ²⁶N. Kosugi, *J. Comput. Phys.* **55**, 426 (1984).